MolecularMedicine

Underexpressed CNDP2 Participates in Gastric Cancer Growth Inhibition through Activating the MAPK Signaling Pathway

Zhenwei Zhang,[1,2] Lei Miao,[3*] Xiaoming Xin,[3,4] Jianpeng Zhang,[1] Shengsheng Yang,[1] Mingyong Miao,[1] Xiangping Kong,[2] and Binghua Jiao[1]*

[1]Department of Biochemistry and Molecular Biology, Second Military Medical University, Shanghai, China; [2]Key Laboratory of Liver Disease, Center of Infectious Diseases, Guangzhou 458 Hospital, Guangzhou, China; [3]Department of Pharmacology, School of Pharmacy and Institute of Biomedical Sciences, Fudan University, Shanghai, China; and [4]Department of Pharmacology, Taishan Medical University, Shandong Province, China

Increasing evidence suggests that cytosolic non-specific dipeptidase 2 (CNDP2) appears to do more than just perform an enzymatic activity; it is functionally important in cancers as well. Here, we show that the expression of CNDP2 is commonly downregulated in gastric cancer tissues. The ectopic expression of CNDP2 resulted in significant inhibition of cell proliferation, induction of cell apoptosis and cell cycle arrest, and suppressed gastric tumor growth in nude mice. We further revealed that the reintroduction of CNDP2 transcriptionally upregulated p38 and activated c-Jun NH_2-terminal kinase (JNK), whereas the loss of CNDP2 increased the phosphorylation of extracellular signal–related kinase (ERK). These results suggest that CNDP2 acts as a functional tumor suppressor in gastric cancer via activation of the mitogen-activated protein kinase (MAPK) pathway.

Online address: http://www.molmed.org
doi: 10.2119/molmed.2013.00102

INTRODUCTION

Gastric cancer, the fourth most common malignancy and the second leading cause of cancer-related death worldwide, is mostly the result of genetic and epigenetic alterations during its progression (1,2). It is well known that understanding the mechanisms in gastric carcinogenesis through the identification and characterization of tumor suppressor genes and oncogenes is crucial to understanding tumor pathogenesis and will help to discover novel targets for therapies (3).

The mitogen-activated protein kinases (MAPKs), for which activities are regulated by Ras/Raf expression, are mainly composed of three serine/threonine-related protein kinases: extracellular signal–related kinases (ERKs), c-Jun NH_2-terminal kinases (JNKs) and p38 MAPKs. Generally, the ERK signaling pathway is typically associated with cell survival, proliferation and differentiation and protecting cells against apoptosis, whereas the JNK and p38 cascades are usually involved in promoting cell growth and apoptosis (4). It has been shown that abnormal MAPK expression is correlated with tumorigenesis and metastatic potential for gastric cancer (5). Thus, identifying new tumor suppressor genes or oncogenes that participate in the MAPK pathway could lead to the discovery of new therapies for gastric cancer.

Cytosolic non-specific dipeptidase 2 (CNDP2), also known as carboxypeptidase of glutamate-like (CPGL), is expressed in all human tissues, and its isoform is CPGL-B, which lacks exons 3 and 4 (6). The *cndp2* gene that translates a dinuclear metalloproteases has 39.5% homology to peptidase family M20 and may belong to the M20A subfamily (6,7). Previously, Zhang *et al.* (7) observed that the isoform CPGL-B is downregulated in hepatocellular cancer and could inhibit the viability, colony formation and invasion of hepatocellular carcinoma cells. A recent report also demonstrated that the loss of CNDP2 functioned as a tumor suppressor gene in pancreatic cancer and that the loss of CNDP2 and CPGL-B

*ZZ and LM contributed equally to this work.

Address correspondence to *Xiangping Kong, Key Laboratory of Liver Disease, Center of Infectious Diseases, Guangzhou 458 Hospital, Dongfengdonglu #801, Guangzhou, 510600, China. Phone: +86-20-87395343; Fax: +86-20-87371180; E-mail: xiangping_kong@hotmail.com; or Binghua Jiao, Department of Biochemistry and Molecular Biology, Second Military Medical University, Shanghai 200433, China. Phone: +86-21-81870970-8001; Fax: +86-21-65334333; E-mail: jiaobh@live.cn.*

Submitted September 7, 2013; Accepted for publication December 17, 2013; Epub (www.molmed.org) ahead of print December 24, 2013.

suppressed proliferation, induced G0/G1 accumulation and inhibited the migration ability of a pancreatic cancer cell line (8). However, not all tumors express a low CNDP2 level, and the molecular function of CNDP2 is largely unknown. Okamura *et al.* (9) showed through quantitative proteomic analysis that renal cell carcinoma tissues have a high level of CNDP2 expression. Tripathi *et al.* (10) found that CNDP2 was upregulated in breast cancer tissues compared with normal breast epithelium. In light of these discrepant results, this study was designed to explore whether there is an aberrant expression of CNDP2 in gastric cancer and to analyze what biological and molecular mechanisms of CNDP2 affect gastric cancer development.

MATERIALS AND METHODS

Cells and Reagents

The following human gastric cancer cell lines were used: AGS was purchased from American Type Culture Collection (Manassas, VA, USA); MKN45, N87 and HGC-27 were obtained from China Center for Type Culture Collection (Wuhan, China); and MKN28, SGC-7901, MGc-803, BGC-823 and GES were provided by the Institute of Biochemistry and Cell Biology of the Chinese Academy of Science (Shanghai, China). All of the cells were maintained in RPMI 1640 (Biowest, Maine et Loire, France) medium supplemented with 10% fetal bovine serum (Biowest), 100 U/mL penicillin, 100 μg/mL streptomycin sulfate and 1 mmol/L sodium pyruvate at 37°C in 5% CO_2.

Clinical Samples

A total of 182 gastric cancer tissues and their corresponding nonneoplastic gastric mucosal tissues were obtained during surgery from Shanghai Changhai Hospital (Shanghai, China). The collection of these tissue samples was undertaken with approval of the Shanghai Changhai Hospital Institutional Review Board and with the patients' informed consent. The tissue microarray (TMA) was constructed as described previously (11).

Immunohistochemical Analysis

Immunohistochemical staining was performed with an EnVision Kit (Dako, Carpinteria, CA, USA). The slices were incubated with primary antibody against CNDP2 (Proteintech, Chicago, IL, USA). The control staining of CNDP2 was conducted by substituting phosphate-buffered saline (PBS) for the primary antibody. The analysis of the immunohistochemical staining was performed independently by two pathologists (Wang Wang, Department of Pathology, Changhai Hospital; Guoliang Qiao, Department of Pathology, Eastern Hepatobiliary Surgery Hospital). Sections were considered positive for CNDP2 when >5% of tumor cells were stained in the cell cytoplasm. The staining intensity was visually graded as negative (–), weak (+), moderate (++) or strong (+++). For each pair sample, CNDP2 was referred to be underexpressed when the carcinoma displayed a weaker staining intensity than its adjacent normal tissue; otherwise, when the carcinoma displayed an equal or stronger staining intensity than its adjacent normal tissue, the CNDP2 expression was taken to be normal.

Plasmid Construction and Cell Transfection

The CNDP2 expression plasmid was constructed by cloning the full-length *cndp2* (Gene Bank accession number NM_018235) open reading frame into the mammalian expression vector GV142 with *Xho*I and *Hind*III restriction enzyme sites (Genechemgene, Shanghai, China). The sequences were verified by DNA sequencing.

AGS cells were transfected with GV142-CNDP2 or empty vector GV142 by using X-tremeGENE HP DNA Transfection Reagent (Roche [F. Hoffmann-La Roche AG, Basel, Switzerland]) according to the manufacturer's instructions. The plasmid expressing GFP was used to evaluate the transfection efficacy. G418-resistant (Sigma-Aldrich, St. Louis, MO, USA) colonies at a concentration of 0.9 mg/mL were selected, and the transfected clones were used for further studies after 14 d of selection.

Lentiviral Vector Silence Construction and Cell Transfection

Three different CNDP2-specific target sequences were chosen by using the CNDP2 reference sequence (NM_018235). Double-stranded DNA were synthesized according to the structure of a GV112 (hU6-MCS-CMV-Puromycin) viral vector (Genechemgene) and then inserted into a linearized vector. The positive clones were identified as the lentiviral vectors named 8856, 8857 and 8858. Among the three vectors, 8857 (target sequence: 5′-ACT TTG ACA TAG AGG AGT T-3′) induced the highest levels of downregulation. Thus, the 8857 vector and viral packaging system were cotransfected into 293 cells to replicate competent lentivirus. The lentivirus containing the human CNDP2 shRNA (short hairpin RNA)-expressing cassette was used as a positive control for lentivirus production and denoted as Lesh-CNDP2 in the subsequent experiments. The GV112 mock vector was packaged and used as a negative control, denoted as Lesh-NC (Lesh–negative control), which has no significant homology to human gene sequences.

SGC7901 cells (30–50% confluence) were transduced with lentiviral vectors Lesh-CNDP2 or Lesh-NC at a multiplicity of infection of 20 in serum-free growth medium containing 5 μg/mL polybrene for 12 h. Then, the cells were washed and cultured continually. The cells were cultured until they reached 70–80% confluence. Next, 2.5 μg/mL puromycin was added to cells, and they were cultured for 48 h to generate a stable transfection cell line.

Reverse Transcription Polymerase Chain Reaction and Quantitative Real-Time Polymerase Chain Reaction Analyses

Total RNA was isolated from frozen human gastric tissues with the TRIzol

method, according to the manufacturer's protocol. One microgram of total RNA was used for cDNA synthesis with the RevertAid™ First-Strand cDNA Synthesis Kit #1622 (Fermentas, Vilnius, Lithuania). The appropriate forward and reverse primers to detect the transcripts of interest were used in reverse transcription polymerase chain reactions (RT-PCRs) for cDNA amplification. The primer sequences for glyceraldehyde-3-phosphate dehydrogenase (GAPDH) were as follows: 5′-CAA GGT CAT CCA TGA CAA CTT TG-3′ (forward) and 5′-GTC CAC CAC CCT GTT GCT GTA G-3′ (reverse). The primer sequences for CNDP2 were as follows: 5′-AAT GGG TGG CTA TCC AGA GT-3′ (forward) and 5′-CAC ATC CAG GTG CCC GTA-3′ (reverse). The PCR conditions used for the amplification were as follows: 94°C for 5 min and then 30 cycles of 94°C for 30 s, 57°C for 30 s and 72°C for 40 s, followed by 72°C for 10 min. The RT-PCR products were analyzed on a 1% agarose gel and visualized with ethidium bromide staining. The gene *GAPDH* was used as a positive control to assess cDNA quality.

Quantitative real-time polymerase chain reaction (Q-RT-PCR) was performed with a 7300 Real-Time PCR System (Applied Biosystems/Life Technologies, Carlsbad, CA, USA). For the semiquantification of the genes of interest, we used the QPK-201 SYBR Green master mix (Toyobo, Osaka, Japan). Target cDNA-specific primers of CNDP2, as described above, were established. The quantity of the target was normalized against the quantity of GAPDH.

Western Blot Analysis

Protein was extracted with radioimmunoprecipitation assay lysis buffer, and Western blots were performed as described previously (12). The following primary antibodies were used: caspase 3, cleaved caspase 3 (c-caspase 3), Bcl-2, Bax, Bad, cyclin E, cyclin B1, cdc2, p38, phospho-ERK1/2 (p-ERK1/2), ERK1/2, phospho-JNK (p-JNK) and JNK (Cell Signaling Technology, Danvers, MA, USA), CNDP2 (Proteintech) and GAPDH (Bioworld Technology Inc, St. Louis Park, MN, USA). The blots were visualized with a horseradish peroxidase–conjugated antibody followed by chemoluminescence reagent (Millipore, Billerica, MA, USA) detection on photographic film. For quantification, the target protein was normalized to the internal standard protein GAPDH through a comparison of the gray scale values; this analysis was performed with Gel Pro Analyzer software, version 4.0 (Media Cybernetics Inc., Rockville, MD, USA).

Cell Viability Assay

Cell viability was measured by a cell counting kit-8 assay (CCK-8; Dojindo, Kumamoto, Japan). Briefly, AGS cells (5×10^3 per well) and SGC-7901 cells (3×10^6 per well) were seeded in 96-well plates and transfected with GV142-NC or GV142-CNDP2 and Lesh-NC or Lesh-CNDP2, respectively. After transfection for 24, 48 or 72 h, the CCK-8 reagents were added and incubated with the cells for 1 h. Then, the absorbance was detected at 450 nm according to the manufacturer's instruction. The experiments were performed in triplicate.

Colony Formation Assay

Colony formation assays were performed as described previously (13). In short, stably transfected AGS and SGC-7901 cells were cultured in six-well plates (500 per well) for 2 wks. The colonies with cell numbers of >50 cells were fixed in cold-methanol and stained with crystal violet solution. The colonies were counted with the Quantity One software (Bio-Rad Laboratories Inc., Hercules, CA, USA) and photographed. All the experiments were performed in triplicate wells in three independent experiments.

Cell Apoptosis and Cell Cycle Analysis

AGS cells transiently transfected with GV142-NC or GV142-CNDP2 and SGC-7901 cells transiently transfected with Lesh-NC or Lesh-CNDP2 were harvested 48 h after transfection. Each transfected cell group was divided into two parts; one portion was processed for cell apoptosis analysis and the second portion for cycle analysis.

Cell apoptosis was assessed with an annexin V–fluorescein isothiocyanate (AV-FITC) apoptosis detection kit. The collected cells were suspended in binding buffer, and AV and propidium iodide (PI) working solutions were added to the cellular suspension in sequence. Then, the stained cells were analyzed with the FACSCalibur flow cytometry system (BD Biosciences, San Jose, CA, USA). The early and late apoptotic cells were counted for relative apoptotic changes. The experiments were performed in triplicate.

To determine the cell cycle distribution, the collected transfected cells were fixed in 70% ethanol at 4°C overnight. Then, the cells were labeled with PI in the presence of RNase A. The fractions of the cells in the G0/G1, S and G2/M phases were analyzed by flow cytometry. All the experiments were performed three times.

Measurement of Reactive Oxygen Species Generation

Intracellular reactive oxygen species (ROS) production was detected with the peroxide-sensitive fluorescent probe 2′,7′-dichlorofluorescin diacetate (DCFH-DA) according to the manufacturer's protocol. Briefly, transiently transfected AGS cells were harvest 48 h after transfection and suspended in 1 mmol/L DCFH-DA at 37°C for 30 min. After treatment with DCFH-DA, the cells were washed twice with PBS and resuspended in PBS for the detection of ROS accumulation using the flow cytometer at a wavelength pair of 488/538 nm. The experiment was repeated three times independently.

In Vivo Tumorigenicity

AGS cells (7.8×10^6 cells in 0.2 mL PBS) stably transfected with GV142-NC, GV142-CNDP2 or untreated control and SGC-7901 cells (3×10^6 cells in 0.2 mL PBS) stably transfected with Lesh-NC or Lesh-CNDP2 were separately injected

subcutaneously into the right flank of nude mice. On d 21, the mice were killed, and the tumor tissues were weighed. The following formula was used for tumor volume measurement: tumor volume = $L \times W^2/2$ (L is length and W is width). The Ethical Committee of the Second Military Medical University approved the current study.

Statistical Analysis

The data were expressed as the mean ± standard deviation (SD). All calculations were performed with SPSS version 11.7. The statistical analyses were performed with a Student *t* test and analysis of variance. Pearson χ^2 test was applied to study the relationship between different variables. All *p* values were two-tailed, and $p < 0.05$ was considered statistically significant.

RESULTS

Somatic Loss of CNDP2 in Gastric Cancer

Immunohistochemical data were obtained from the tissue array that consisted of 182 pairs of samples, primary gastric cancer tissues and corresponding adjacent nontumor regions. A total of 132 (72.53%) tumor tissue samples exhibited a lower level of CNDP2 expression than the matched adjacent normal tissues, whereas the 50 pairs of samples showed nearly no difference of CNDP2 expression between the carcinomas and the adjacent tissues (Figure 1A). The association between the CNDP2 protein underexpression and clinicopathological factors of a gastric cancer patient was analyzed by Pearson χ^2 test and is shown in Table 1. The somatic loss of CNDP2 in gastric cancer was significantly associated with tumor site ($p = 0.016$), tumor type ($p = 0.013$), disease stage ($p = 0.044$) and pathologic T stage (pT) ($p = 0.01$). There was, however, no association between the reduced CNDP2 expression and patient sex, patient age, tumor size or tumor pathologic N stage (pN).

Additionally, CNDP2 mRNA expression was investigated in gastric cancer with RT-PCR and Q-RT-PCR. The two analyses revealed that CNDP2 mRNA expression was significantly reduced in gastric cancer tissues relative to the matched adjacent nontumor tissues (Figures 1B, C). Furthermore, the loss of CNDP2 expression was also confirmed by Western blot in paired gastric carcinoma tissues and nonpaired gastric cancer tissues (Figure 1D). Collectively, these results demonstrate that CNDP2 expression, at either the protein or mRNA level, was significantly attenuated in gastric cancer tissues compared with the matched adjacent nontumor tissues and that the loss of CNDP2 expression may be associated with the tumorigenesis of gastric cancer.

CNDP2 Varies Expression in Gastric Cancer Tissues and Epithelial Cell Lines

Next, we examined CNDP2 protein levels in different differentiated grades of gastric adenocarcinoma tissues. As shown in Figure 1E, CNDP2 expression decreased after the decrease of differentiation degree. Furthermore, the expression of CNDP2 in the gastric cancer cell lines AGS, MKN28, SGC-7901, MKN45, MGc80-3, BGC-823, N87 and HGC-27 and the human immortalized gastric mucosa epithelial cell line GES was determined by Q-RT-PCR and Western blot. Of these cell lines, the poorly differentiated adenocarcinoma cell lines AGS, MGc80-3 and BGC-823 exhibited relatively low levels of CNDP2 expression, whereas the other poorly differentiated MKN45 cell line revealed relatively high protein levels of CNDP2, but low mRNA level. Although the well-differentiated adenocarcinoma cell line N87 exhibited relatively low levels of CNDP2, the moderately differentiated adenocarcinoma cell line SGC-7901, the undifferentiated adenocarcinoma cell line HGC-27 and gastric epithelial cell line GES revealed significantly high CNDP2 levels (Figures 1F, G). Collectively, these results indicate that CNDP2 expression is varied following the differentiation degree of gastric cancer tissues or epithelial cell lines, at least to some extent.

Upregulated CNDP2 Inhibits Gastric Cancer Growth *In Vitro* and *In Vivo*

To address the potential role of CNDP2 in the tumorigenesis of gastric cancer, AGS cells with low CNDP2 expression were transfected with the GV142-CNDP2 or GV142 vector. The upregulated expression of CNDP2 was shown at two time points by Western blot (Figure 2A). Ectopic CNDP2 expression dramatically suppressed cell growth in CNDP2-transfected cells compared with the control vector transfectants (Figure 2B). Additionally, the inhibitory effect on cell growth was confirmed by colony formation assay, which showed CNDP2 inhibited the number of colonies in AGS cells (Figure 2C). We further examined whether CNDP2 could suppress the growth of AGS cells *in vivo* by evaluating tumor development in nude mice. GV142-CNDP2 and GV142-NC stably transfected AGS cells, and untreated control cells were injected subcutaneously into the flank of immunodeficient mice. As shown in Figure 2D, tumor growth was significantly decreased in CNDP2-transfected nude mice compared with the untreated control and vector-transfected mice. In addition, the tumor masses and tumor volume both indicated that the tumorigenic activity of AGS cells was significantly inhibited when CNDP2 expression was upregulated (Figure 2E). Thus, these results suggest that ectopic CNDP2 expression inhibits tumor growth in gastric cancer.

Loss of CNDP2 Enhances Gastric Cancer Growth

To further substantiate the functional significance of CNDP2 in gastric cancer, SGC-7901 cells, which express a high level of CNDP2, were transfected with the lentiviral vector silencing construct. The CNDP2 protein level was dramatically reduced in Lesh-CNDP2 versus Lesh-NC transfectants (Figure 3A). Next, the effects of CNDP2 knockdown on SGC-7901 cell proliferation were evaluated by CCK-8 assays. As shown in Figure 3B, silencing CNDP2 expression significantly promoted cell growth in CNDP2-transfected cells compared with

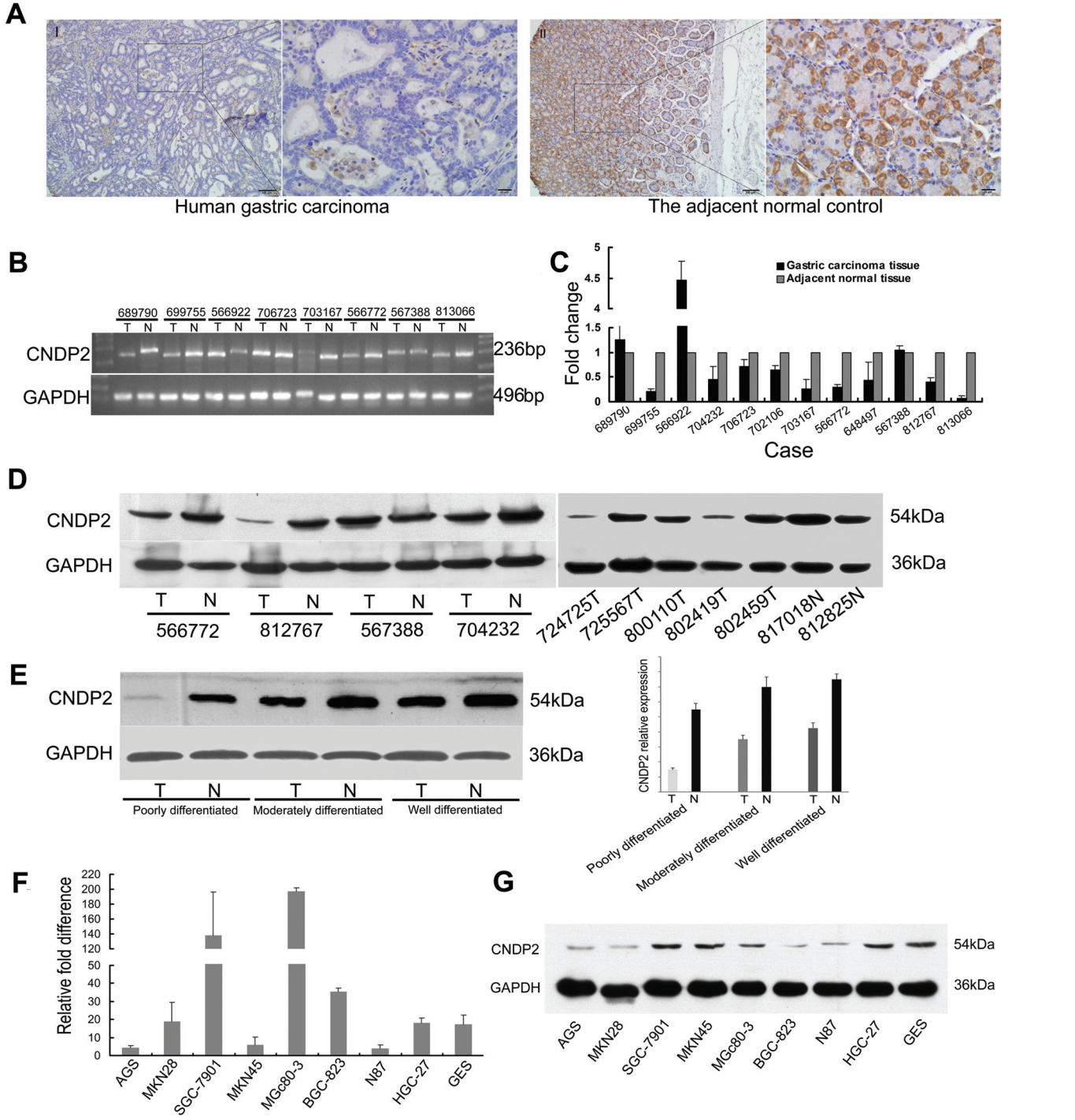

Figure 1. CNDP2 expression is downregulated in human gastric cancer. (A) Immunohistochemical staining of CNDP2 in human gastric cancer and adjacent normal specimens. Negative CNDP2 staining in gastric cancer tissues (I) and positive CNDP2 staining in the matched adjacent normal tissues (II) is shown. (B, C) RT-PCR and Q-RT-PCR showed that CNDP2 expression was downregulated in gastric cancer tissues compared with the matched adjacent nontumor tissues. (D) Western blot indicated that CNDP2 expression was downregulated in paired gastric cancer tissues and nonpaired gastric cancer tissues. T, tumor tissues; N, surrounding nontumor tissues. (E) CNDP2 protein levels were analyzed in gastric adenocarcinoma tissues with different differentiation degree. (F, G) Analysis of CNDP2 expression in human gastric carcinoma cell lines. Q-RT-PCR and Western blot revealed that the expression of CNDP2 varies in gastric cancer epithelial cell lines.

Table 1. Correlation between CNDP2 expression and clinicopathological characteristics.

	Underexpression of CNDP2 (n (%))	Normal expression of CNDP2 (n (%))	*p*
Sex			0.855
Male	89 (67.4)	33 (66)	
Female	43 (32.6)	17 (34)	
Age (years)			0.07
>60	62 (47)	31 (62)	
≤60	70 (53)	19 (38)	
Tumor size (cm)			0.638
<6	79 (59.8)	28 (56)	
≥6	53 (40.2)	22 (44)	
Site			0.016
Cardia and fundus	35 (26.5)	5 (10)	
Corpus	34 (25.8)	20 (40)	
Antrum	63 (47.7)	25 (50)	
Type			0.013
Tubular adenocarcinoma	38 (28.8)	26 (52)	
Mucosal adenocarcinoma	43 (32.6)	10 (20)	
Signet-ring cell carcinoma	51 (38.6)	14 (28)	
Disease stage			0.044
I and II	47 (35.6)	26 (52)	
III and IV	85 (64.4)	24 (48)	
pT stage			0.01
T0–T2	37 (28)	5 (10)	
T3 and T4	95 (72)	45 (90)	
pN stage			0.193
N0	42 (31.8)	11 (22)	
N1–3	90 (68.2)	39 (78)	
Total	132	50	

the control and vector transfectants. Additionally, the colony formation assay also showed that the Lesh-CNDP2-transfected cells possessed a significantly higher colony forming efficiency (Figure 3C). Similar to the stably transfected AGS cells, Lesh-CNDP2 and Lesh-NC stably transfected SGC-7901 cells were also injected subcutaneously into the immunodeficient mice to verify the tumor growth inhibition of CNDP2. Interestingly, the lentiviral-mediated CNDP2 silencing resulted in a significantly higher amount of tumor growth in the xenograft model than in the lentiviral vector control (Figure 3D). Statistically, the tumor masses and volume of the two transfectant groups both showed that the decreased expression of CNDP2 facilitates tumor growth in nude mice (Figure 3E). Taken together, these results indicate that CNDP2 functions as a tumor suppressor in gastric carcinogenesis.

CNDP2 Induces Apoptosis, Cell Cycle Rest and the ROS Generation

To determine the mechanism underlying the CNDP2-induced tumor suppression, cell apoptosis, cell cycle and ROS were assessed by flow cytometry. The results showed that the upregulation of CNDP2 expression resulted in a significant increase in early apoptotic cells compared with the vector only and untreated control in AGS cells (Figure 4A). Additionally, CNDP2-transfected AGS cells revealed higher G0/G1 phase populations in comparison with the empty vector transfectants and untreated control (Figure 4B). Similar to the cell apoptosis and cell cycle analyses, the ROS generation of AGS cells transfected with GV142-CNDP2 was also calculated. The ectopic expression of CNDP2 exhibited a significant increase in ROS generation, as shown in Figure 4C. In addition, the effects of CNDP2 knockdown on cell apoptosis and cell cycle were also explored in SGC-7901 cells. However, it is interesting to note that the apoptotic cell death in Lesh-CNDP2–transfected cells was not significantly different from Lesh-NC–transfected cells (Figure 4D). Furthermore, CNDP2 silencing did not induce a change in the cell cycle distribution (Figure 4E). Regardless, these results suggest that the inhibition of gastric carcinogenesis by CNDP2 may partly involve cell apoptosis, G0/G1 phase arrest and ROS induction.

CNDP2 Activates the MAPK Signaling Pathways

To further validate the flow cytometry results that showed tumor growth inhibition was suppressed by CNDP2, apoptosis and cell cycle protein markers were detected in AGS and SGC-7901 cells, respectively, 48 h after they were transfected with CNDP2. Western blot detection of CNDP2 clearly confirmed a significant increase of protein levels in AGS cells that were transfected with GV142-CNDP2 and a significant decrease in SGC-7901 cells transfected with Lesh-CNDP2. Also, the results showed c-caspase 3 and Bax were upregulated and Bcl-2 was downregulated, but Bad was unaffected in CNDP2-transfected AGS cells compared with the vector-transfected and untreated controls. These four proteins remained unchanged when the expression of CNDP2 was knocked down in SGC-7901 cells (Figure 5A). Moreover, the induction of cell cycle arrest was further evidenced by the decreased expression of cyclin E, a key G0/G1 phase arrest factor, but not in the expression of cyclin B1 and cdc2, in CNDP2-transfected AGS cells. The expression of these three cell cycle–related proteins, however, was unchanged in the Lesh-CNDP2–transfected SGC-7901 cells (Figure 5A). Therefore, these data corroborate the arguments that the induction of cell apoptosis and cell cycle arrest by CNDP2 may play an important role in the process of gastric carcinogenesis.

Considerable evidence indicates that MAPK signaling cascades possess dual

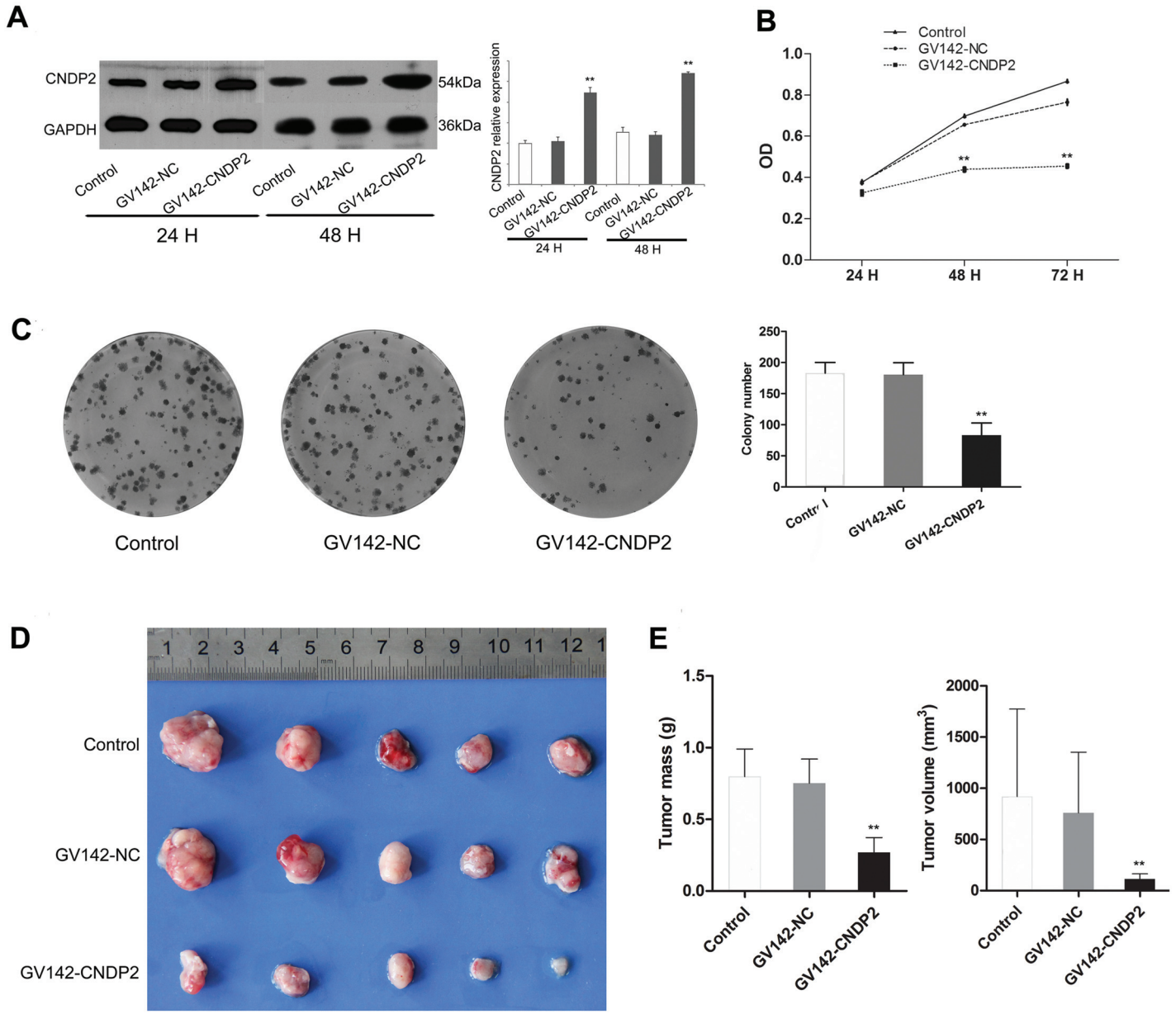

Figure 2. Effect of ectopic CNDP2 expression on tumor growth. (A) CNDP2 protein levels were assessed by Western blot in AGS cells. A marked increase in CNDP2 was evident in GV142-CNDP2 transfectants relative to the untreated control and GV142-NC transfectants. (B) Cell proliferation levels were measured by the CCK-8 assay. GV142-CNDP2 transfectants displayed significantly inhibited growth rates in AGS cells. (C) The upregulated expression of CNDP2 significantly inhibited the colony formation of AGS cells. (D) Ectopic CNDP2 expression decreased tumor growth in nude mice subcutaneously inoculated with AGS/GV142-CNDP2 compared with the untreated control and AGS/GV142-NC *in vivo*. (E) The tumor masses and tumor volume for three groups are compared; each histogram represents the mean ± SD of five mice. $^{**}p < 0.01$ from the GV142-NC group.

functions: stimulation and inhibition of cell growth (14,15). To elucidate the molecular mechanisms modulated by CNDP2 in tumor inhibition, the role of CNDP2 in the activation of p38, ERK1/2 and JNK MAPK was determined. Figure 5A showed that p38 and p-JNK levels increased and p-ERK1/2, ERK1/2 and JNK levels remained unchanged when CNDP2 was upregulated. However, the data also showed that only the expression of p-ERK1/2 was enhanced after CNDP2 silencing. To further substantiate the activation of MAPK pathway that CNDP2 induced *in vivo*, the activation of ERK, JNK and p38 in CNDP2-transfected xenograft tissues was revealed by Western blot. Consistent with *in vitro*, the results

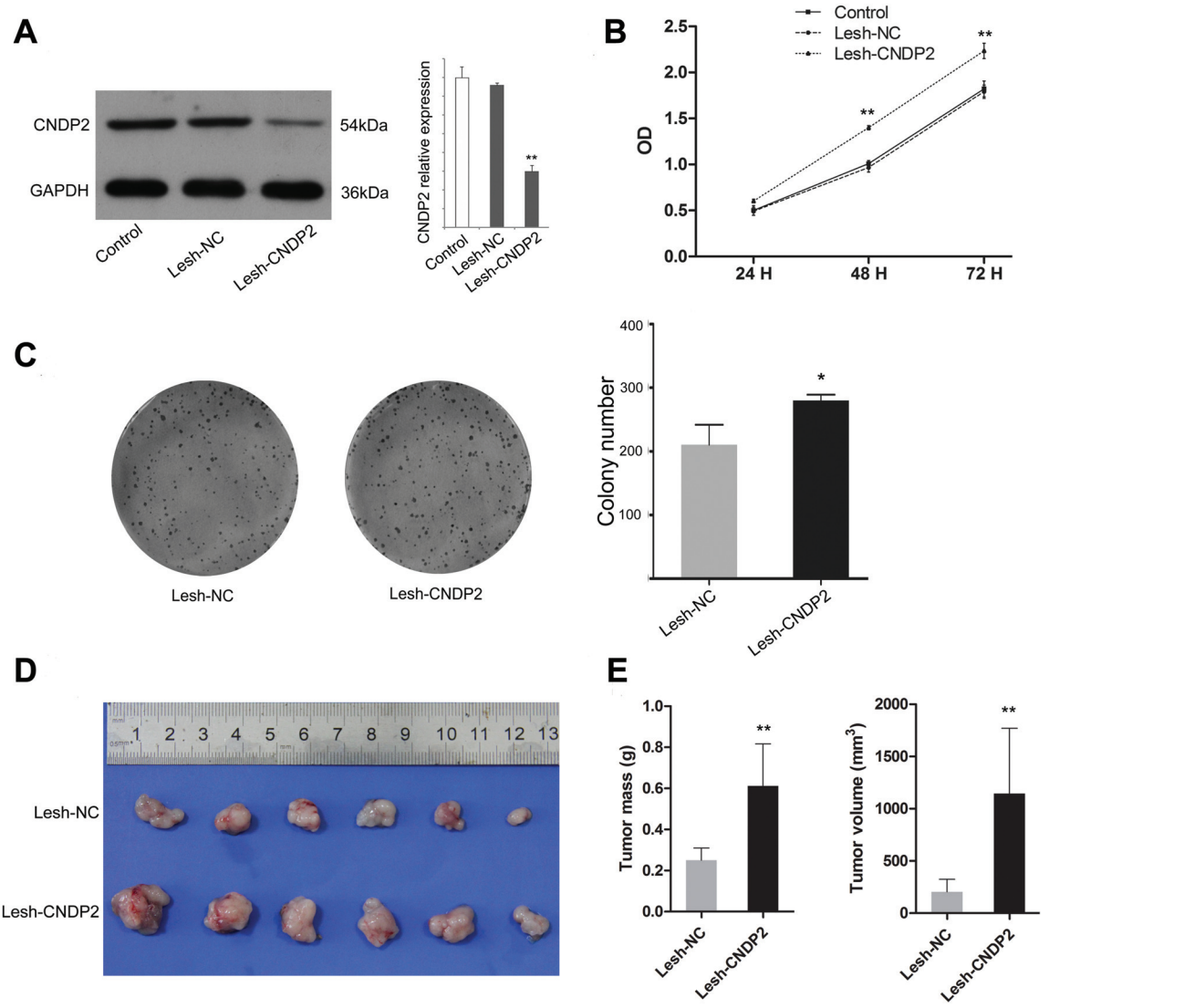

Figure 3. CNDP2 knockdown promotes tumor growth *in vitro* and *in vivo*. (A) CNDP2 protein levels were analyzed in SGC-7901 cells. A significant reduction of CNDP2 level was observed in Lesh-CNDP2 transfectants compared with the Lesh-NC transfectants and untreated control. (B) The cell proliferation levels were measured by the CCK-8 assay. Lesh-CNDP2 transfectants had significantly increased growth rates in SGC-7901 cells. (C) Lesh-CNDP2 transfected cells possessed significantly higher colony-forming efficiency. (D) CNDP2 silencing facilitated tumor growth in nude mice subcutaneously inoculated with SGC-7901/Lesh-CNDP2 compared with SGC-7901/Lesh-NC *in vivo*. (E) The tumor masses and tumor volume for the two groups are compared, and the bar graph shows the mean tumor masses or volume for Lesh-CNDP2 (n = 6) and Lesh-NC (n = 6) transfectants. *$p < 0.05$, **$p < 0.01$, from the Lesh-NC group.

showed that both p38 and p-JNK were upregulated in CNDP2 overexpressed xenograft tissues, whereas only p-ERK1/2 was activated when CNDP2 was silencing (Figure 5B). Taken together, these results indicate that CNDP2 may induce cell apoptosis via the p38 and JNK MAPK signaling pathways and suppress cell proliferation through the ERK MAPK signaling pathway, at least in specific circumstances.

DISCUSSION

CNDP2 and its homolog, CNDP1, which is secreted and preferentially expressed in the brain, are dinuclear metalloproteases that belong to the M20 family and have been shown to possess carnosine (β-alanyl-L-histidine) peptidase activity (6,16). CNDP2 encodes a nonspecific dipeptidase that cleaves some dipeptides with high affinity such as Cys-Gly of the γ-glutamyl cycle, participating in glutathione biosynthesis (17,18). In addition, recent advances have demonstrated that CNDP2 is overexpressed in substantia nigra compacta tissue and may be a new key player in the molecular mechanisms of neurodegeneration underlying Parkinson's disease (18). However, accumulating evidence indicates that the dipeptidase

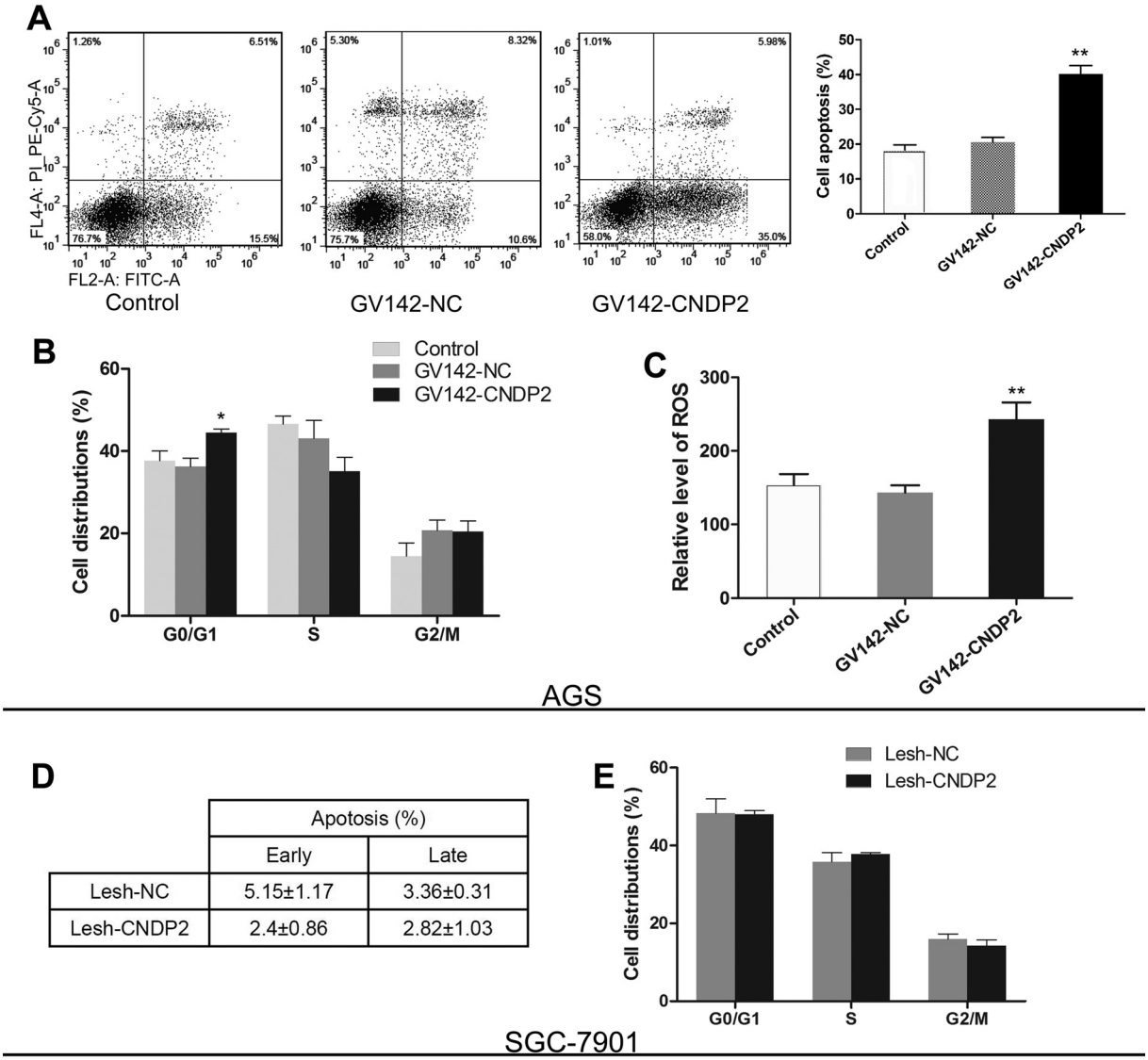

	Apotosis (%)	
	Early	Late
Lesh-NC	5.15±1.17	3.36±0.31
Lesh-CNDP2	2.4±0.86	2.82±1.03

Figure 4. Effects of CNDP2 on the cell apoptosis, cell cycle and ROS generation of gastric cancer cells. (A) The rate of cell apoptosis 48 h after AGS cells were transfected with CNDP2 was determined by flow cytometry. Statistical analysis of the percentages of the apoptotic cells. The experiments were performed in duplicate. (B) Cell cycle distribution was analyzed by FACS flow cytometry in AGS cells 48 h after they were transfected with GV142-CNDP2 or GV142-NC. The cell cycle distribution percentage shown is from three independent experiments. (C) AGS cells that were stably transfected with CNDP2 were loaded with DCFH-DA. The mean DCF fluorescence was measured. And the histograms are representative of the percentage of DCF fluorescence of three independent experiments. *$p < 0.05$, **$p < 0.01$, from the GV142-NC group. (D) The table reports the percentages of apoptotic SGC-7901 cells 48 h after they were transfected with Lesh-CNDP2 or Lesh-NC. (E) The cell cycle distribution was analyzed 48 h after SGC-7901 cells were transfected with Lesh-CNDP2 or Lesh-NC. The cell cycle distribution percentage shown is from three independent experiments.

appears to do more than just perform its enzymatic activity. The protein was found to be upregulated in breast and renal cell carcinoma (9,10). Furthermore, it has been suggested that CNDP2 has distinct patterns of expression within grades in kidney cancer (19). There has been a lack of direct evidence, however, as to what role CNDP2 plays in these cancers. Two reports bring new and notable possibilities that CNDP2 functions as a tumor suppressor gene and plays important roles in the tumorigenesis of hepatocellular and pancreatic cancer (7,8). Nevertheless, these apparently divergent functions of CNDP2 in tumor progression are currently difficult to reconcile, but could reflect its important effects in cancer. Sorting out the exact roles of CNDP2 in different cancers will be important.

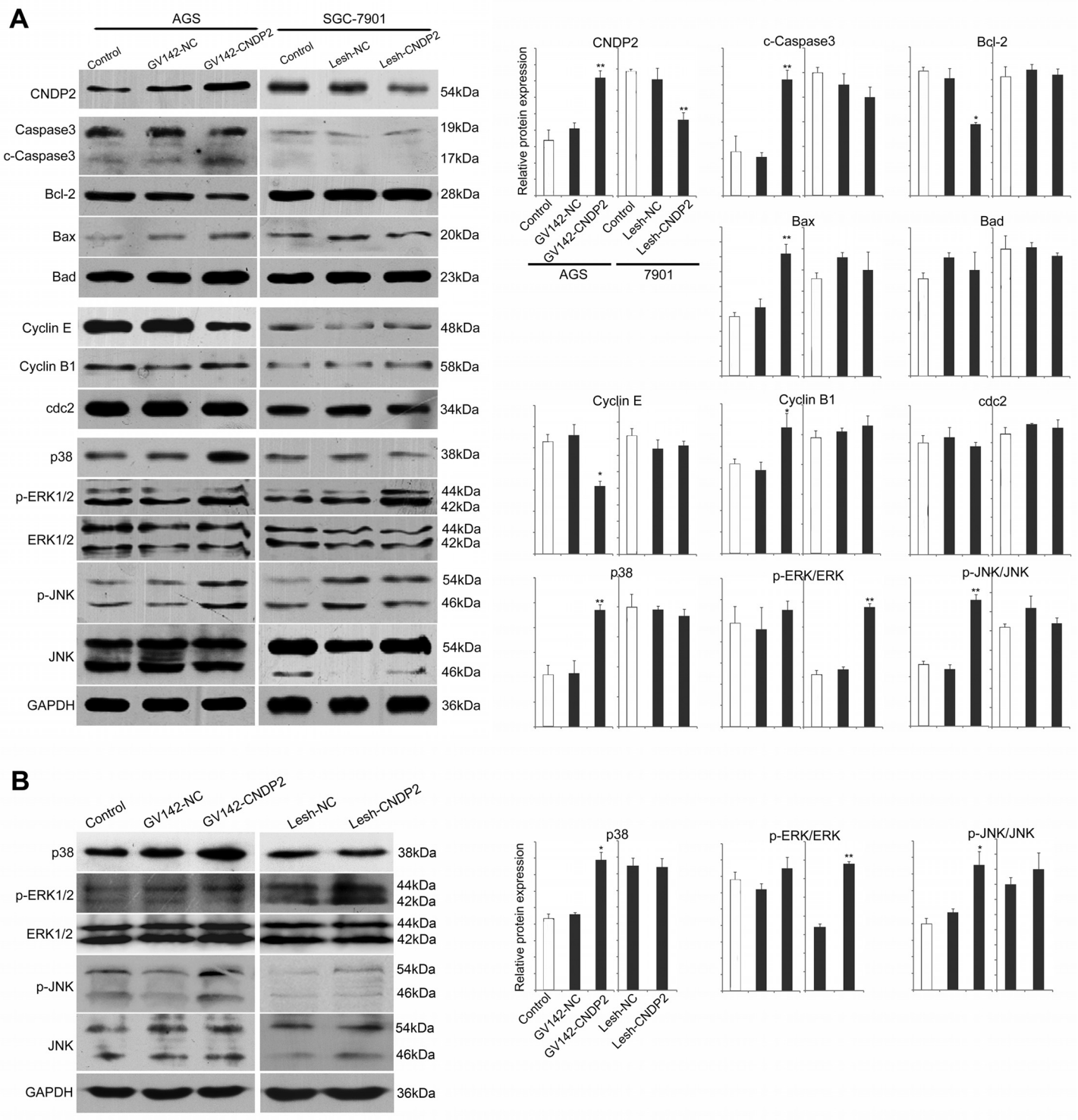

Figure 5. Effects of CNDP2 on protein markers of apoptosis, the cell cycle and the MAPK pathways. (A) Protein indicators related to apoptosis (caspase 3, c-caspase 3, Bcl-2, Bax, Bad), the cell cycle (cyclin E, cyclin B1, cdc2) and the MAPK pathways (p38, p-ERK1/2, ERK1/2, p-JNK, JNK) were detected by Western blot 48 h after AGS, and SGC-7901 cells were transfected with CNDP2. GAPDH was used as the loading control. (B) The effects of CNDP2 on protein markers of MAPK pathways were assessed by Western blot in tumor xenograft tissues. $^{*}p < 0.05$, $^{**}p < 0.01$, from the GV142-NC or Lesh-NC group.

Thus, on the basis of similar reports of the downregulation of CNDP2 and its isoform CPGL-B in hepatocellular and pancreatic carcinoma involving tumor growth inhibition, we hypothesized that CNDP2 could be aberrantly expressed in gastric cancer and might serve as a tumor suppressor gene or oncogene in gastric carcinogenesis.

We have shown that the downregulation of CNDP2 is a common event during gastric tumorigenesis. In gastric cancer tissues and epithelial cell lines, the expression of CNDP2 decreased accordingly with the decrease of differentiation, which is in line with the report that CNDP2 exerted grade-dependent changes in kidney cancer (19). The ectopic expression of CNDP2 in the AGS cells, which express a low level of CNDP2, displayed significant growth suppression resulting from the inhibition of cell proliferation and colony formation. The diminution of tumor growth by CNDP2 was further confirmed by reduced tumorigenesis in a mouse xenograft model. On the other hand, lentiviral-mediated knockdown of CNDP2 in the SGC-7901 cells that express a high level of CNDP2 significantly increased cell proliferation and tumorigenesis in nude mice. Thus, our present study clearly demonstrates that the tumor suppressor role of CNDP2 extends far beyond its enzymatic activity and highlights the critical importance of CNDP2 as a tumor suppressor gene in gastric carcinogenesis.

The role of tumor suppressor genes in carcinogenesis have traditionally been attributed to their ability to regulate the cell cycle and sustain proliferative signaling while also helping cells evade growth suppression and/or cell death (20,21). Thus, analyzing the effects of CNDP2 on cell apoptosis and the cell cycle of gastric cancer cells may further our understanding of the function of CNDP2 in cancer. Our results showed that the ectopic expression of CNDP2 in AGS cells significantly increased early cell apoptosis. This result was confirmed by the upregulation of cleaved caspase 3 and Bax and by the downregulation of Bcl-2. Cleaved caspase 3 is the executor of cell death, and an elevated Bax/Bcl-2 ratio corresponds with cell apoptosis (21,22). Additionally, ROS generation also verified the increase in cell apoptosis (23). Besides apoptosis, CNDP2 also induced the G0/G1 phase cell cycle arrest of AGS cells. Cyclin E is required for the transition from the G1 to S phase of the cell cycle, which determines cell division. The decrease in cyclin E, but not cyclin B1 or cdc2, indicated that there was an accumulation of cells in the G0/G1 phase (24). Moreover, we checked these results in SGC-7901 cells that have a downregulated level of CNDP2 expression. The silencing of CNDP2 promoted cell proliferation, but did not change the cell apoptosis or cell cycle distribution. On the other hand, the apoptosis-related and cell cycle–related proteins both remained unchanged when CNDP2 was silencing. This result may be the reason that loss of CNDP2 enhances SGC-7901 cell growth and the growing cells contain few apoptotic- and cell cycle–arrested cells.

To further demystify the role of CNDP2 in gastric carcinogenesis, we elucidated in which downstream signaling pathways CNDP2 exerts a tumor suppressor function during gastric cancer and found that CNDP2 activated the MAPK signaling pathway. Significant attention has been given to the important role of the MAPK pathway and the several key components and phosphorylation events that play a role in regulating the cell cycle, apoptosis and even tumorigenesis (14). Our results showed that elevated CNDP2 expression was accompanied by increases in the synthesis of p38 and p-JNK, whereas the loss of CNDP2 induced p-ERK aggregation, indicating a direct influence of CNDP2 on the activation of the MAPK signaling pathway. And such observations also suggest that the MAPK pathway that is involved in the CNDP2-induced tumor growth suppression may be regulated differently. Among the MAPK subfamilies, the activation of the ERK pathway has long been associated with proliferation, growth and the apoptotic signaling pathways, in some cases (25). The p38 and JNK pathways are generally responsible for the apoptotic response induced by several DNA-damaging agents (26). When CNDP2 was under its normal level, the inhibitory property of the dipeptidase was declined and the ERK pathway was activated then. However, under the scenario that CNDP2 was abundant, the protein level of p38 and p-JNK increased, and then the gastric carcinogenesis was possibly retardant. Therefore, it is plausible that the inhibitory properties of MAPK against gastric cancer cell growth observed in this study could be explained, at least in part, by an elevated level of CNDP2, which activates the p38 and JNK MAPK pathways to induce cell apoptosis, and by downregulated CNDP2, which activates the ERK MAPK pathway to promote cell proliferation.

CONCLUSION

Altogether, our study underscores an important role for CNDP2 as a candidate tumor suppressor gene that is epigenetically silenced in gastric cancer. The molecular biological and cell biological analyses of CNDP2 suggest that the dipeptidase contributes to the suppression of tumorigenesis by decreasing cell proliferation and inducing cell apoptosis and cell cycle arrest through the activation of the MAPK signaling pathway. Therefore, our novel observations may provide additional support for the hypothesis that CNDP2 is a potent negative tumor regulator and establish a strong rationale for developing CNDP2 as a viable therapeutic regimen to treat gastric cancers.

DISCLOSURE

The authors declare that they have no competing interests as defined by *Molecular Medicine*, or other interests that might be perceived to influence the results and discussion reported in this paper.

REFERENCES

1. Ushijima T, Sasako M. (2004) Focus on gastric cancer. *Cancer Cell.* 5:121–5.
2. Hartgrink HH, Jansen EP, van Grieken NC, van de Velde CJ. (2009) Gastric cancer. *Lancet.* 374:477–90.
3. Bayani J, *et al.* (2007) Genomic mechanisms and measurement of structural and numerical instability in cancer cells. *Semin. Cancer Biol.* 17:5–18.
4. Johnson GL, Lapadat R. (2002) Mitogen-activated protein kinase pathways mediated by ERK, JNK, and p38 protein kinases. *Science*. 298:1911–2.
5. Liang B, *et al.* (2005) Increased expression of mitogen-activated protein kinase and its upstream regulating signal in human gastric cancer. *World J. Gastroenterol.* 11:623–8.
6. Teufel M, *et al.* (2003) Sequence identification and characterization of human carnosinase and a closely related non-specific dipeptidase. *J. Biol. Chem.* 278:6521–31.
7. Zhang P, *et al.* (2006) Identification of carboxypeptidase of glutamate like-B as a candidate suppressor in cell growth and metastasis in human hepatocellular carcinoma. *Clin. Cancer Res.* 12:6617–25.
8. Lee JH, *et al.* (2012) Loss of 18q22.3 involving the carboxypeptidase of glutamate-like gene is associated with poor prognosis in resected pancreatic cancer. *Clin. Cancer Res.* 18:524–33.
9. Okamura N, *et al.* (2008) Quantitative proteomic analysis to discover potential diagnostic markers and therapeutic targets in human renal cell carcinoma. *Proteomics.* 8:3194–203.
10. Tripathi A, *et al.* (2008) Gene expression abnormalities in histologically normal breast epithelium of breast cancer patients. *Int. J. Cancer.* 122:1557–66.
11. Yu G, *et al.* (2009) Overexpression of phosphorylated mammalian target of rapamycin predicts lymph node metastasis and prognosis of Chinese patients with gastric cancer. *Clin. Cancer Res.* 15:1821–9.
12. Zhang Z, *et al.* (2012) Interleukin-11 promotes the progress of gastric carcinoma via abnormally expressed versican. *Int. J. Biol. Sci.* 8:383–93.
13. Zhang Z, *et al.* (2012) Wentilactone B from Aspergillus wentii induces apoptosis and inhibits proliferation and migration of human hepatoma SMMC-7721 cells. *Biol. Pharm. Bull.* 35:1964–71.
14. Santarpia L, Lippman SM, El-Naggar AK. (2012) Targeting the MAPK-RAS-RAF signaling pathway in cancer therapy. *Expert. Opin. Ther. Targets.* 16:103–19.
15. Wagner EF, Nebreda AR. (2009) Signal integration by JNK and p38 MAPK pathways in cancer development. *Nat. Rev. Cancer.* 9:537–49.
16. Otani H, Okumura N, Hashida-Okumura A, Nagai K. (2005) Identification and characterization of a mouse dipeptidase that hydrolyzes L-carnosine. *J. Biochem.* 137:167–75.
17. Kaur H, *et al.* (2009) Dug1p Is a Cys-Gly peptidase of the gamma-glutamyl cycle of Saccharomyces cerevisiae and represents a novel family of Cys-Gly peptidases. *J. Biol. Chem.* 284:14493–502.
18. Licker V, *et al.* (2012) Proteomic profiling of the substantia nigra demonstrates CNDP2 overexpression in Parkinson's disease. *J. Proteomics.* 75:4656–67.
19. Perroud B, Ishimaru T, Borowsky AD, Weiss RH. (2009) Grade-dependent proteomics characterization of kidney cancer. *Mol. Cell Proteomics.* 8:971–85.
20. Hanahan D, Weinberg RA. (2011) Hallmarks of cancer: the next generation. *Cell.* 144:646–74.
21. Ward PS, Thompson CB. (2012) Metabolic reprogramming: a cancer hallmark even Warburg did not anticipate. *Cancer Cell.* 21:297–308.
22. Antonsson B, *et al.* (1997) Inhibition of Bax channel-forming activity by Bcl-2. *Science.* 277:370–2.
23. Li Z, Yang Y, Ming M, Liu B. (2011) Mitochondrial ROS generation for regulation of autophagic pathways in cancer. *Biochem. Biophys. Res. Commun.* 414:5–8.
24. Hinds PW, *et al.* (1992) Regulation of retinoblastoma protein functions by ectopic expression of human cyclins. *Cell.* 70:993–1006.
25. Okano J, Rustgi AK. (2001) Paclitaxel induces prolonged activation of the Ras/MEK/ERK pathway independently of activating the programmed cell death machinery. *J. Biol. Chem.* 276:19555–64.
26. Shen HM, Liu ZG. (2006) JNK signaling pathway is a key modulator in cell death mediated by reactive oxygen and nitrogen species. *Free Radic. Biol. Med*. 40:928–39.